


RESEARCH

Open Access



320 cardiac MDCT angiography in preoperative assessment of TOF and its variants: Does it worth it?

Eman Abdel Sadek Taha Elreweny^{1*} , Mohammed Mahmoud Dawoud¹, Alaa Basiouni Said Mahmoud², Mohamed A. Amin¹ and Hossam Mohammed Abdel Hafiz Zaitoun¹

Abstract

Background: Tetralogy of Fallot is the most common cyanotic congenital heart disease encountering a large spectrum of anatomical presentations with differing surgical approaches, and long-term outcomes ranging from ventricular septal defect with limited aortic overriding and mild pulmonary obstruction to a critical form of VSD and pulmonary atresia. TOF variants include PA/VSD, TOF/CAVC, TOF/DORV and TOF with absent pulmonary valve. Also, it may be accompanied with many associated intracardiac and extracardiac anomalies that may be of value when imaging and planning the surgical procedure.

Results: Our study included 22 cases of classic TOF, 18 with PA/VSD (12 were of type A, 5 were of type B and 1 was of type C), 3 with TOF/CAVC and 7 TOF/DORV. Sub-valvular RVOTO was detected in 94% of patients. A statistically significant difference was depicted between Echocardiography and MDCT in detecting supra-valvular RVOTO, however no statistically significant difference was found in sub-valvular and valvular RVOTO detection. MDCT could efficiently characterize pulmonary arterial tree with statistically significant difference between both Echocardiography and MDCT in assessment of main, right and left pulmonary arteries with P value = 0.036, 0.014 and 0.023 respectively. With calculation of Mc-Goon ratio in all patients, it was favorable (> 1.2) in 33 patients (66%). MDCT entailed 19 patients with PDA versus 15 depicted by Echocardiography and 25 MAPCAs per 11 patients compared 8 MAPCAs per 7 patients detected by Echocardiography. Right sided aortic arch was found in 10 patients and 24 patients showed abnormal branching pattern. Coronary artery abnormalities were identified in eight patients. MDCT showed 100% sensitivity and 100% specificity in depicting aortic, coronary and other associated extracardiac vascular anomalies.

Conclusion: MDCT offers comprehensive anatomical assessment of TOF, and its variants providing superiority over echocardiography and comparable results to cardiac catheterization with 100% sensitivity and specificity in evaluation of associated extracardiac vascular anomalies as well as pulmonary arteries characterization. It is worth using MDCT routinely in combination with echocardiography for the preoperative assessment of TOF and its variants representing a less invasive option than conventional catheterization with lower radiation exposure.

Keywords: TOF, Variants, MDCT, Associated anomalies

Introduction

Tetralogy of Fallot (TOF) is the most common of all cyanotic congenital heart diseases encompassing a large anatomical spectrum with differing surgical approaches and long-term outcomes as well as multiple intellectual and technical challenges. TOF spectrum ranges from

*Correspondence: emanelreweny28@yahoo.com

¹ Radiodiagnosis and Medical Imaging, Faculty of Medicine, Tanta University, El Gharbia, El-geish Street, Tanta, Gharbya Governorate, Egypt
Full list of author information is available at the end of the article

ventricular septal defect (VSD) with limited aortic overriding and mild pulmonary obstruction to a critical form of VSD and pulmonary atresia. Also, it can be associated with common atrioventricular septal defect (CAVC), can be included in the spectrum of double-outlet right ventricle (DORV) or present with a variant form such as TOF with absent pulmonary valve [1, 2]. In addition, there are many associated intracardiac and extracardiac anomalies that must be taken into consideration when imaging and planning the surgical procedure needed [3].

Traditionally, cardiologists have relied on echocardiography and conventional angiography to establish the diagnosis of congenital heart disease [4]. However, they have many limitations that preclude accurate evaluation prior to surgical correction. Small acoustic window of the echocardiography precludes the evaluation of certain anatomical structures (e.g., ascending aorta, aberrant coronary anatomy, pulmonary arteries, and MAPCAs). High cost, ionizing radiation burden, invasive nature, and prolonged sedation anesthesia are the main disadvantages of cardiac catheterization [5].

Excellent anatomic and functional assessment capabilities, high spatial resolution and fast data acquisition make MDCT an obvious modality to evaluate the unstable neonate with a small heart and complex anatomy [6]. With the improved spatial and temporal resolution of MDCT in addition to, and its capacity to produce static as well as 3D reconstructed images of the heart and main vessels, this imaging modality is now one of the main techniques used to assess the anatomy of patients with TOF [1, 7].

In addition, MDCT angiography affords several advantages compared with other current imaging options. When compared with echocardiography, MRI, or conventional angiography, CT provides the most thorough evaluation of the thorax. Sedation is also less frequently necessary than in the other three imaging modalities. The presence of metal artifact is also less of an issue than with MRA. Cost is substantially less than conventional angiography, and procedural risks with conventional angiography must also be a part of the decision process [8].

In this study we investigated role of MDCT in comparison to echocardiography as a diagnostic tool in preoperative assessment of TOF, its variants as well as associated intracardiac and extracardiac anomalies with referral to catheter/operative data as our gold standard.

Methods

Study population

This prospective analytical study was conducted in Radiodiagnosis and Medical imaging Department and included 50 patients referred to from pediatric cardiology and Cardio-thoracic Departments to perform MDCT

cardiac angiography between November 2019 and October 2021. Informed written consents were obtained from the parents of all participants in the study. Consultation with the referring physician and reviewing clinical background of the case were attempted to understand the reason for referral and expectations of the physician from the study.

All the patients had Echocardiographic reports of suspected or diagnosed TOF or one of its variants and underwent MDCT cardiac angiography of the heart and great vessels to confirm the diagnosis or to answer specific anatomic questions raised by inconclusive echocardiography finding before planning the adequate management. Echo and MDCT findings were compared with the data collected by cardiac catheterization and/or operation.

Patients with renal dysfunction (serum creatinine more than 1.5 mg/dL) or serious allergy to iodinated contrast media were excluded from the study. We ensured privacy and confidentiality of all patient's data and their coded numbers.

Cardiac MDCT angiography

Data acquisition

Patients were scanned using 320-row multi-slice CT scanner (Aquilion One, Toshiba Medical Systems, Otawara, Japan). Patients below 5 years ($n=48$) were orally sedated by administration of chloral hydrate ($n=41$) (50–100 mg/kg; maximum dose, 2000 mg) or I.V. administered Midazolam ($n=7$) (0.05–0.1 mg/kg). Older patients ($n=2$) were responding satisfactorily to verbal reassurance and be able to completely suspend respiration.

Non-ionic, non-diluted contrast material (Ultravist 300 or Omnipaque 300) was injected through the peripherally inserted IV cannula (20- to 24- gauge) using dual syringe mechanical power injector (Stellant D, Medrad, Indianola, PA, USA) with contrast volume calculated according to body weight with maximum dose 2 mL/kg, and flow rate 1–1.5 mL/s increased to 3 mL/s in older children followed by IV saline chaser injection of 1 mL/kg. Manual Bolus tracking was applied 10–15 s after contrast material injection (for upper limb venous line) and after 20 s (for lower limb venous line), the scan is initiated after opacification of both ventricles.

All scans were performed in a craniocaudal direction, with CT parameters adapted to the patient's weight. All patients were scanned using retrospective ECG gated CTA volume scan with a rotation time of 0.35 s and a tube voltage of 80 kV increased to 100 kV in older two patients. The tube current ranged from 150 to 450 Ma with automatic dose modulation based on the size and shape of the individual patient. All patients had single

phase image acquisition except for two patients who had additional delayed venous phase scan for better evaluation of the venous anatomy. A case with left isomerism where a delayed phase was obtained to assess systemic and pulmonary venous drainage. The other case was having total anomalous pulmonary venous return (supracardiac type) to assess the ascending vertical vein. After examination, the dose-length product (DLP) was recorded for radiation dose evaluation.

Image reconstruction and post processing

Full volumes were reconstructed in 0.5 mm-thickness slice. Post-processing of multi-slice CT scans including Maximum intensity projections (MIP), three-dimensional volume rendering (VR), multiplanar (MPR) and curved planer reformations (CPR) was performed on a dedicated Vital Images workstation (VitreaFx, vital images, USA).

Image interpretation

After reviewing the axial images, Multiplanar reformations were used as confirmatory tool in the evaluation. Images were interpreted guided by the anatomical and segmental/sequential approach to assess heart including situs, atrio-ventricular and ventriculo-arterial connection, right ventricular outflow Tract (RVOT) assessment, Interventricular septum and Interatrial septum, size and morphology of the cardiac chambers as well as pulmonary circulation, aortic overriding, aortic root rotation, ascending aorta and aortic arch, systemic venous drainage, coronary arteries and anomalous branches crossing the RVOT.

Assessment of image quality:

- The overall image quality of ECG-CTA was rated using a subjective visual score which is a four-point scale system (1–4) in which 4 for excellent (excellent image quality, excellent visualization of anatomic structures), 3 for good (good image quality, clear delineation of anatomic details), 2 for fair (fair image quality, insufficient for complete evaluation), and 1 for poor (poor image quality, uninterpretable anatomic information with severe artifacts) [9, 10].
- Grades 3 or 4 were considered to be sufficient for diagnosis.
- Excellent diagnostic visual score (score 4) was achieved in 39/50 scans (78%), while good diagnostic score (score 3) was achieved in 11/50 scans (22%). The mean image quality score of 50 cases was 3.780 ± 0.418 . None of them was of non-diagnostic image quality.

Radiation dose estimation

The dose-length product (DLP) of each participant was recorded during the examination. The effective dose (ED) was derived from the DLP and a conversion coefficient k ($ED = DLP \times k$). The size of the CTDI phantom was 36 cm. The specific dose length product conversion coefficients for infants were different for different age ranges: less than 4 months, conversion coefficient of 0.039 mSv/(mGy-cm); 4 months to 1 year of age, conversion coefficient of 0.026 mSv/(mGy-cm); 1–6 years, conversion coefficient of 0.018 mSv/(mGy-cm); older than 6 years, conversion coefficient of 0.014 [11, 12].

Statistical analysis

The results were tabulated in a master chart using a Micro-Soft Excel data sheet. Statistical analysis of the present study was performed using SPSS V.20. Qualitative data was presented using number and percentage. Quantitative data resented as mean and standard deviation (SD). For categorical variables Either Chi-square test, Mc-nemar test or Marginal homogeneity test was used for analysis. The level of significance was adopted at $P < 0.05$. Descriptive statistics of each parameter were obtained and compared with similar parameters of other published studies.

Results

Fifty patients were enrolled in this prospective study (26 females and 24 males) with female to male ratio: 52% to 48%. The age group of the study cohort ranged from 4 days to 74 months with mean age 14.430 ± 19.783 and median 10 months. 54% of the patients were diagnosed in the first year of life, only 2 patients were diagnosed ≥ 72 month. 37 patients (74%) presented with cyanosis, cardiac murmurs were heard in 33 patient (66%), 7 patients (14%) had post exercise dyspnea, 5 patients (10%) had irritability, 8 patients (16%) had squatting, only one patient came with failure to thrive. Many patients have more than one presentation.

TOF variants assessed by cardiac MDCT

The examined cases ($n = 50$ cases) were classified according to the findings into classic TOF; TOF with pulmonary stenosis (TOF/PS) ($n = 22$) (Fig. 1), TOF with pulmonary atresia (PA/VSD) variant ($n = 18$) (Fig. 2), TOF with complete atrioventricular canal (TOF CAVC) variant ($n = 3$) (Fig. 3), TOF with double outlet right ventricle (TOF DORV) variant ($n = 7$) (Fig. 4) and TOF absent pulmonary valve variant ($n = 0$).

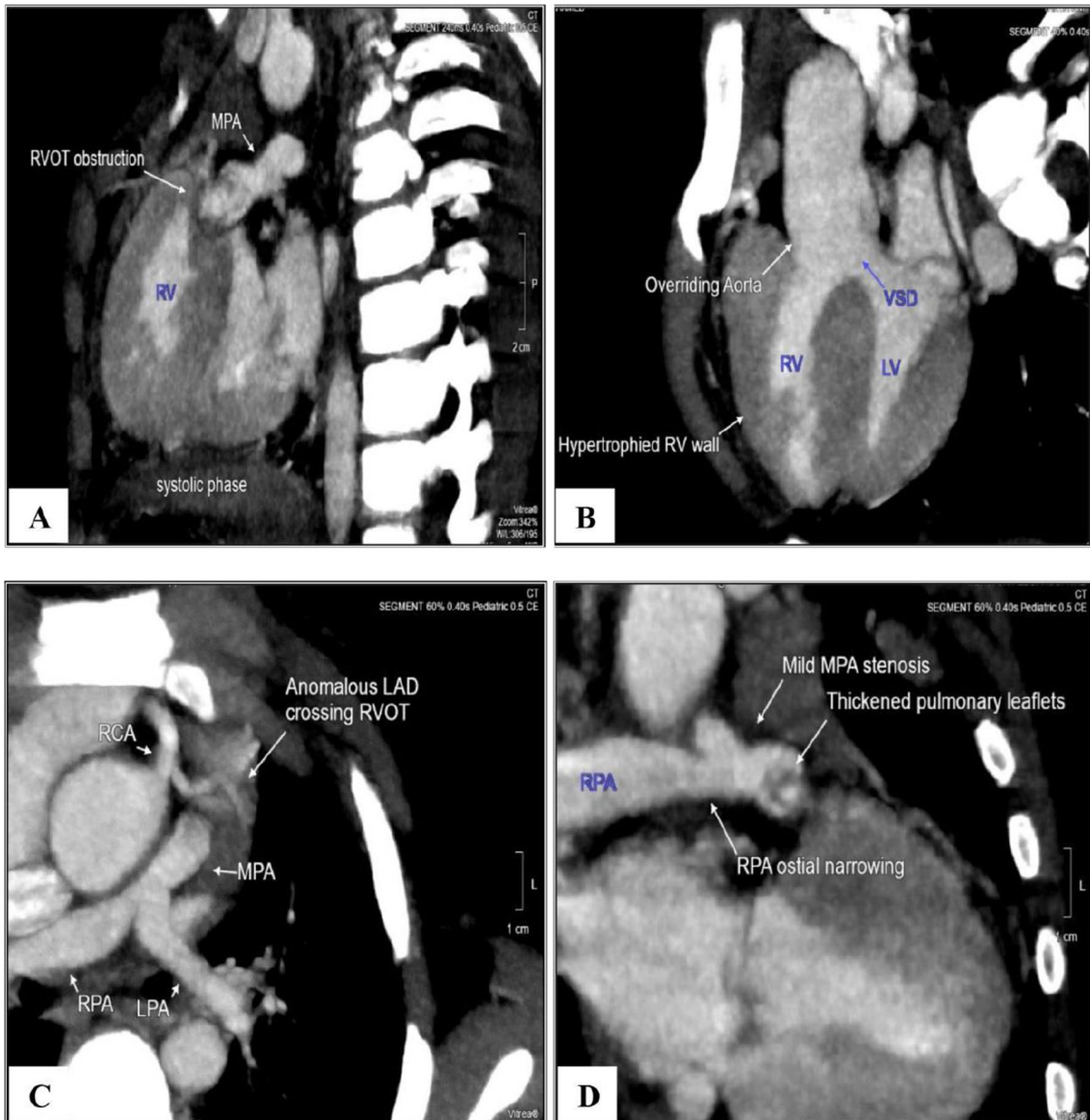


Fig. 1 5 years old girl with classic TOF (TOF/PS) with clinical history of cyanosis. **A** MPR sagittal image showing marked sub-valvular (infundibular) RVOT stenosis. **B** Oblique reformatted image showing Overriding aorta (equal to both ventricles), ventricular septal defect (VSD), dilated ascending aorta and hypertrophied right ventricular wall. **C** Axial MIP image showing distal MPA stenosis and right RPA ostial stenosis. Note Anomalous LAD seen arising from RCA and crossing RVOT. **D** Oblique reformatted MIP image showing thickened pulmonary valve leaflets (valvular stenosis) as well as distal MPA and RPA ostial narrowing. **E** Oblique reconstructed MIP image showing PFO and dilated RA. **F** MPR axial image showing close wise rotation of the aortic root with pre-pulmonic LAD seen originating from RCA and crossing RVOT in addition to another one originating from LM (Dual LAD). **G** VR image anterior view showing Dual LAD with pre-pulmonic LAD seen originating from an ectatic RCA and crossing RVOT in addition to the one originating from LM. **H** VR image posterior view showing RPA ostial narrowing. Note left vertebral artery seen arising from aorta (arrow). **I** VR image of RVOT and pulmonary arterial tree showing distal MPA stenosis and RPA ostial narrowing. Note anomalous LAD from ectatic RCA seen crossing RVOT

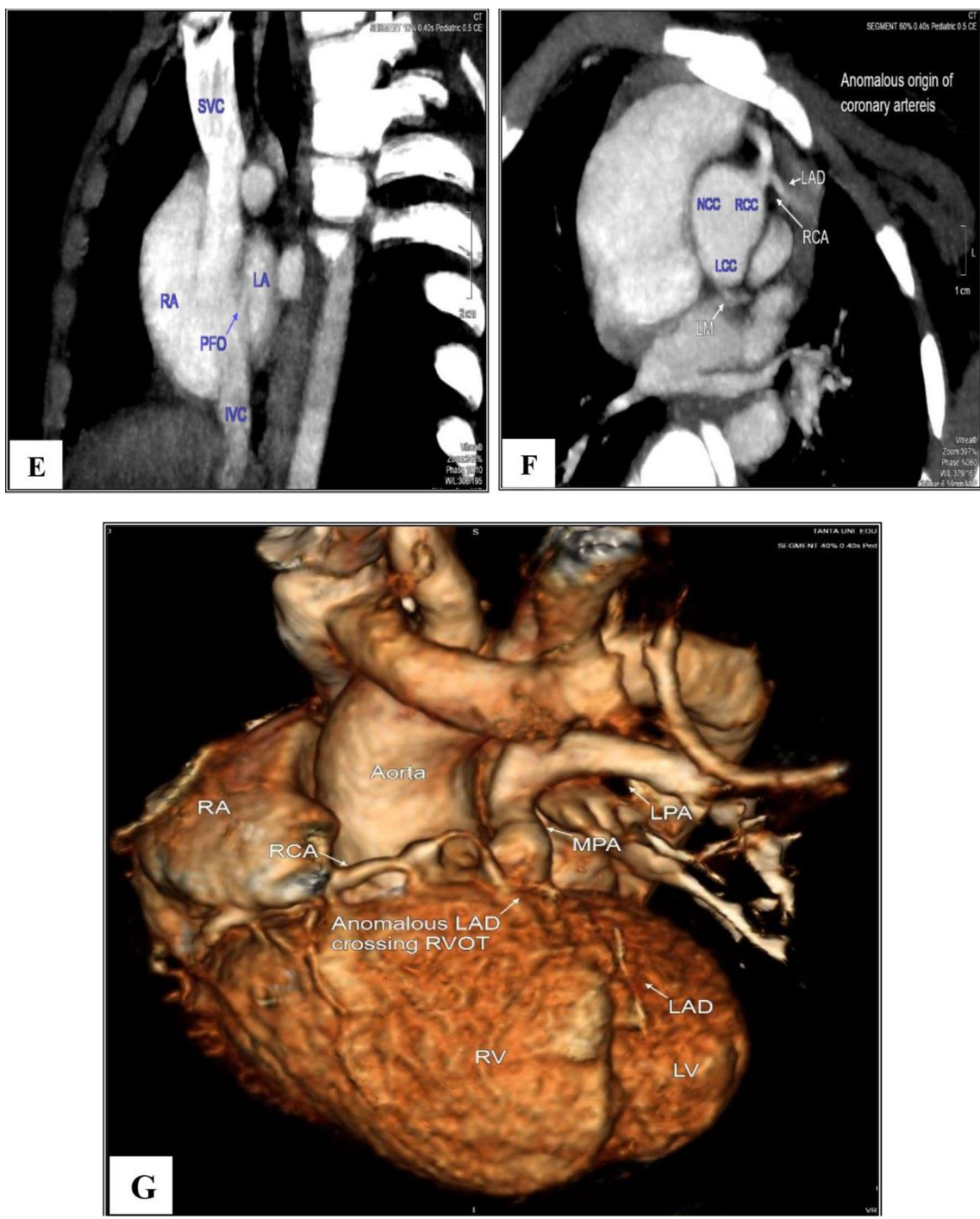


Fig. 1 continued

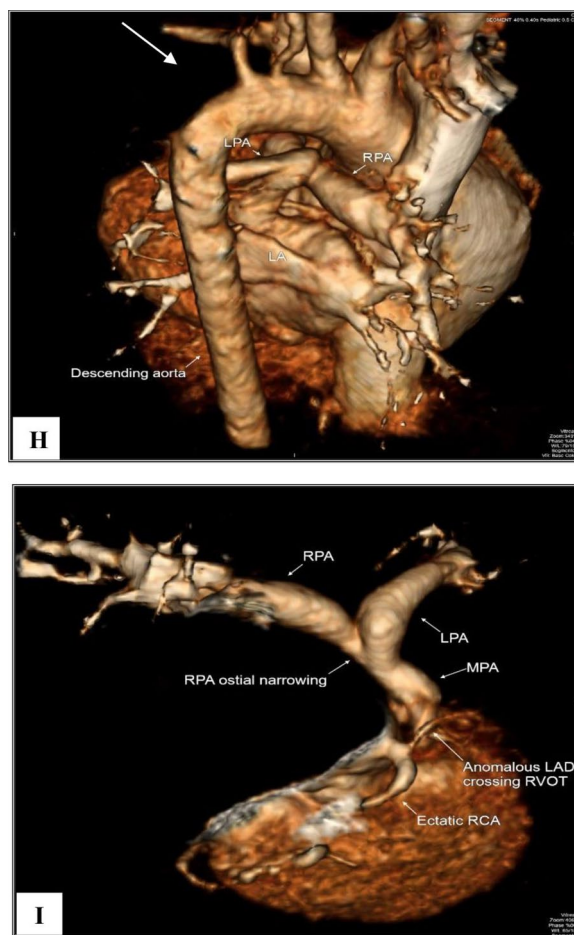


Fig. 1 continued

The eighteen cases of PA – VSD variant were subclassified according to the status of native pulmonary arteries, MAPCAs and PDA to 3 types (A, B and C). Twelve (66.67%) cases were of type A, five (27.78%) cases were of type B (Fig. 2) and only one case was of type C.

Viscero-atrial situs and cardiac position detection

Echocardiography could evaluate the viscerotrial situs correctly in 49 patients (98%) and misdiagnosed one patient (reported as situs solitus by Echocardiography however revealed to be situs ambiguous on MDCT examination). Chi square test revealed non statistically significant difference between both Echo and MDCT in detection of situs ($P=1.000$). All patients had levocardia detected correctly by either Echocardiography and MDCT examination.

TOF cardinal components assessed Echo and cardiac MDCT

Both Echocardiography and MDCT could correctly identify TOF four cardinal components in all patients; interventricular communication, aortic override, Right Ventricular Outflow Tract Obstruction (RVOTO) and right ventricular hypertrophy.

Outlet peri-membranous subaortic VSD was detected in 47 patients (94%) however 3 patients (6%) have large inlet VSD extending to the outlet region (atrioventricular canal type). Both types identified correctly by Echocardiography and MDCT examination. Four patients (8%) have additional VSD, MDCT could correctly identify all of them, however Echocardiography missed diagnosis one of them. No statistically significant difference was detected between Echo and MDCT in detection of VSD ($P=1.000$).

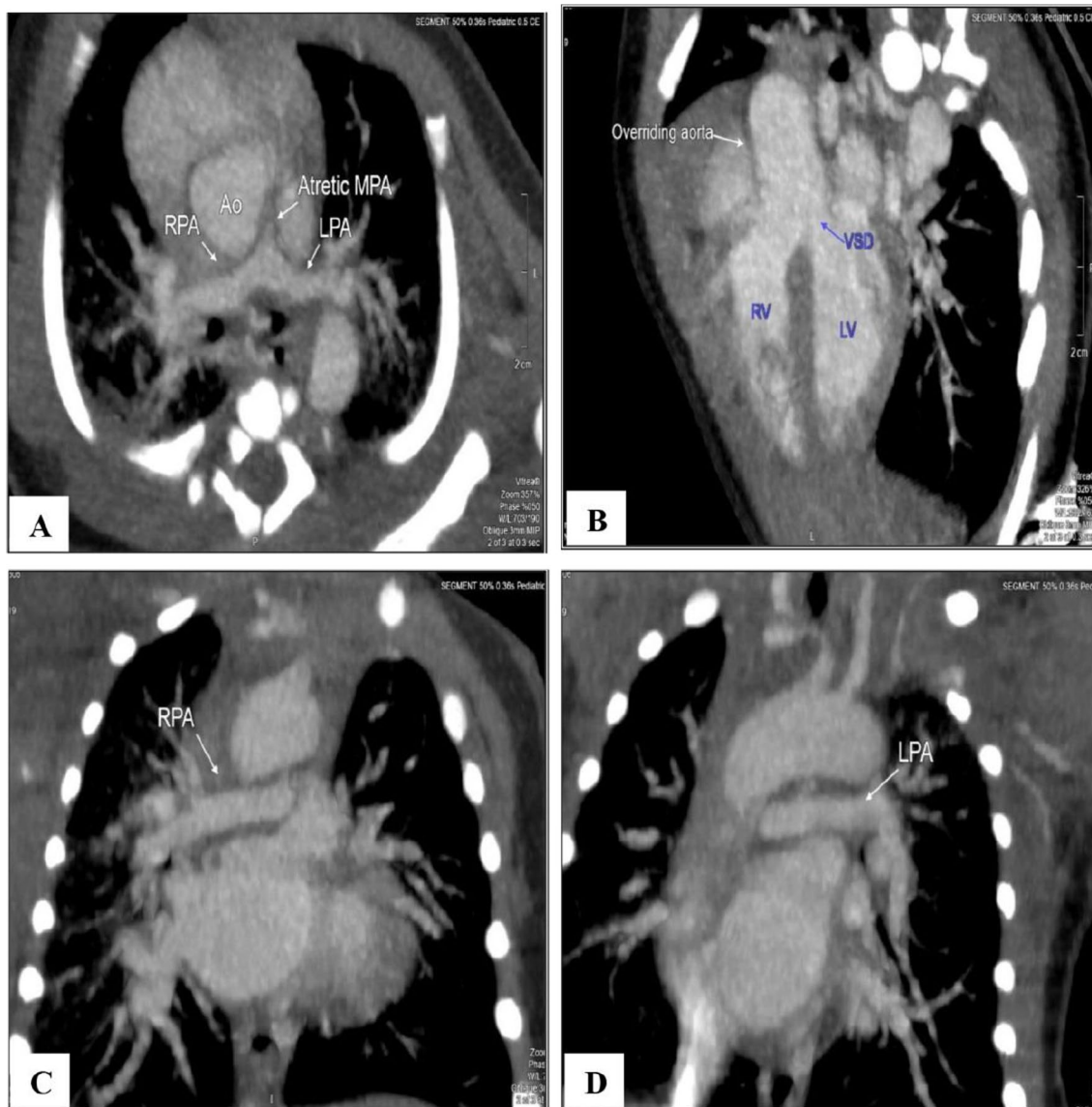


Fig. 2 12 days old girl with TOF/PA variant and MAPCA dependent pulmonary circulation (Type B) presented with cyanosis **A** MPR image showing MPA atresia with hypoplastic both pulmonary branches. **B** Oblique reformatted image showing ventricular septal defect (VSD), Overriding aorta and hypertrophied right ventricular wall. **C, D** MPR images showing hypoplastic pulmonary artery branches. **E, F** MPR sagittal and axial images showing sizeable MAPCA arising from the anterior wall of descending aorta to the lower lobe branch of LPA just distal to LPA bifurcation point. **G** Oblique reconstructed MIP image showing PFO and RA and LA. **H** MPR coronal MIP image showing normal pulmonary venous drainage. **I** VR image of the pulmonary arterial tree showing MPA atresia and hypoplastic confluent pulmonary artery branches. **J** VR image (posterior view) showing sizeable MAPCA arising from descending aorta to the LPA lower lobe branch. **K** VR image (posterior view) showing prominent bronchial artery

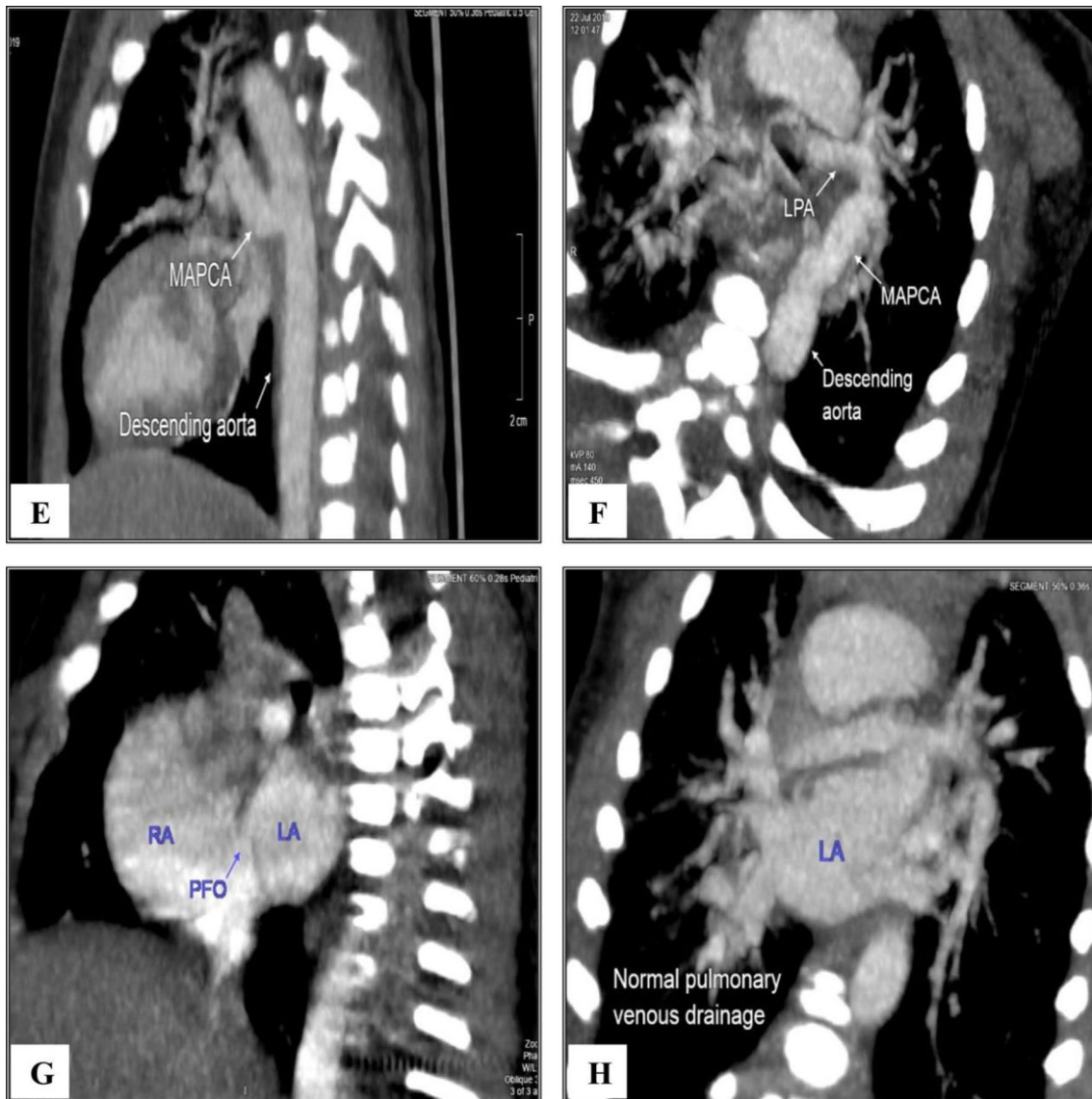


Fig. 2 continued

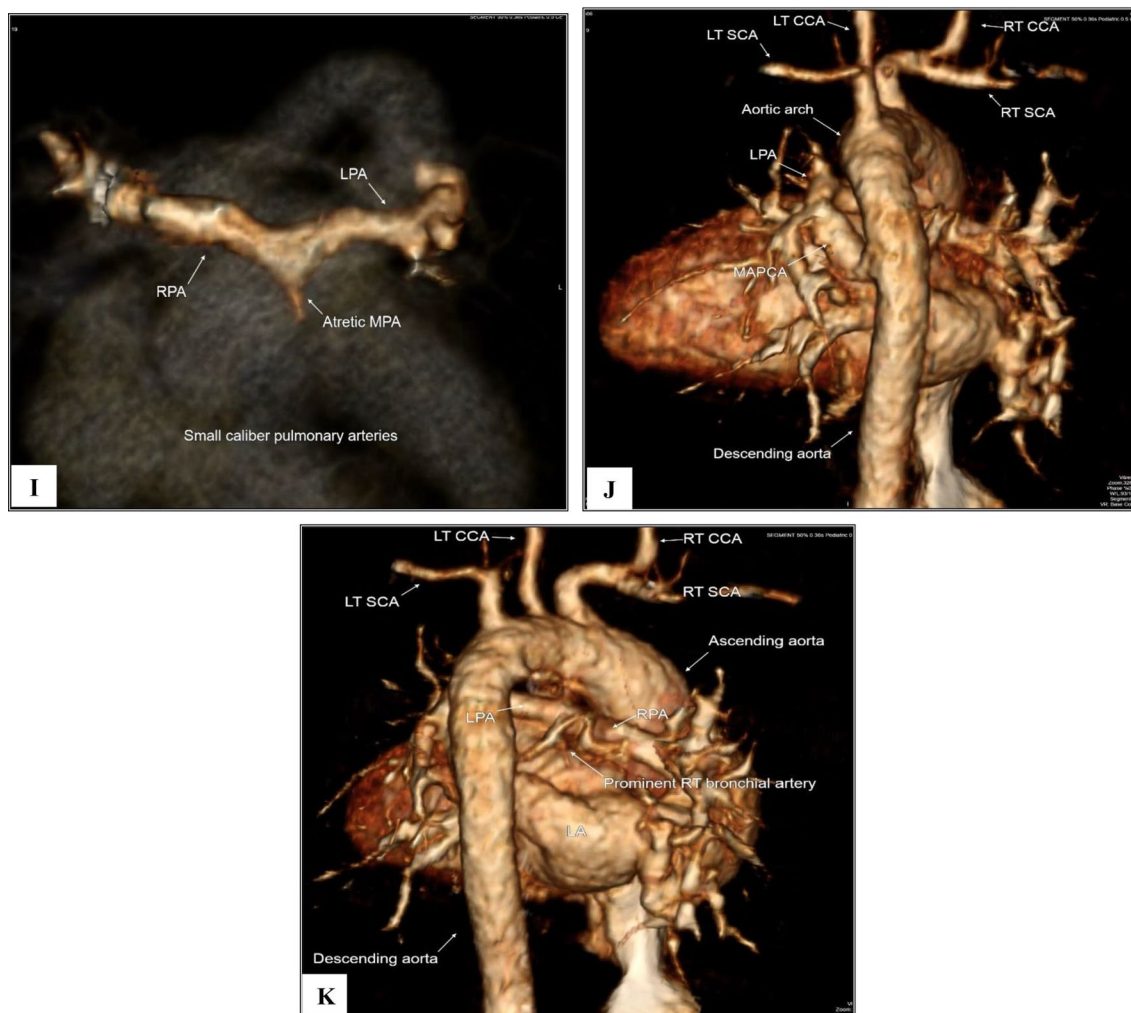


Fig. 2 continued

MDCT and Echocardiography could detect aortic overriding, right ventricular hypertrophy as well as right ventricular outflow obstruction in all patients showing 100% agreement.

RVOTO was classified into sub-valvular, valvular, and supra-valvular levels of obstruction. The valvar level was subdivided into either stenotic or atretic valve and the supra valvular level was subdivided into either central MPA or its branches (right and left pulmonary arteries). Sub-valvular stenosis was detected in 47 patients (94%). Both MDCT and Echo displayed 100% agreement in diagnosis of sub-valvular (infundibular) stenosis. Valvular RVOTO (including valve stenosis or atresia) detected 34 patients (68%) by Echocardiography versus 30 (60%) detected by MDCT. Atretic valve found in 18 patients (36%) with 100% agreement between MDCT and Echocardiography. Less agreement

(92%) between them in detecting stenotic valve. Echocardiography depicted valve stenosis in 16 patients (32%) versus 12 (24%) depicted by MDCT examination. MDCT missed diagnosis of valve stenosis in 4 patients (8%). As regard to supra-valvular level of RVOTO, main pulmonary artery abnormalities (whether hypoplastic, stenotic or atretic MPA) detected in 23 patients (46%) versus 30 (60%) detected by MDCT showing agreement of 86% between them. Echocardiography failed to detect seven patients. Right pulmonary artery abnormalities detected in 10 patients (20%) versus 18 (36%) detected by MDCT showing agreement of 84% between them. Echocardiography failed to detect 8 patients (16%). Left pulmonary artery abnormalities detected in 10 patients (20%) versus 18 patients (36%) detected by MDCT showing agreement of 84%. Echocardiography failed to detect 8 patients (16%).

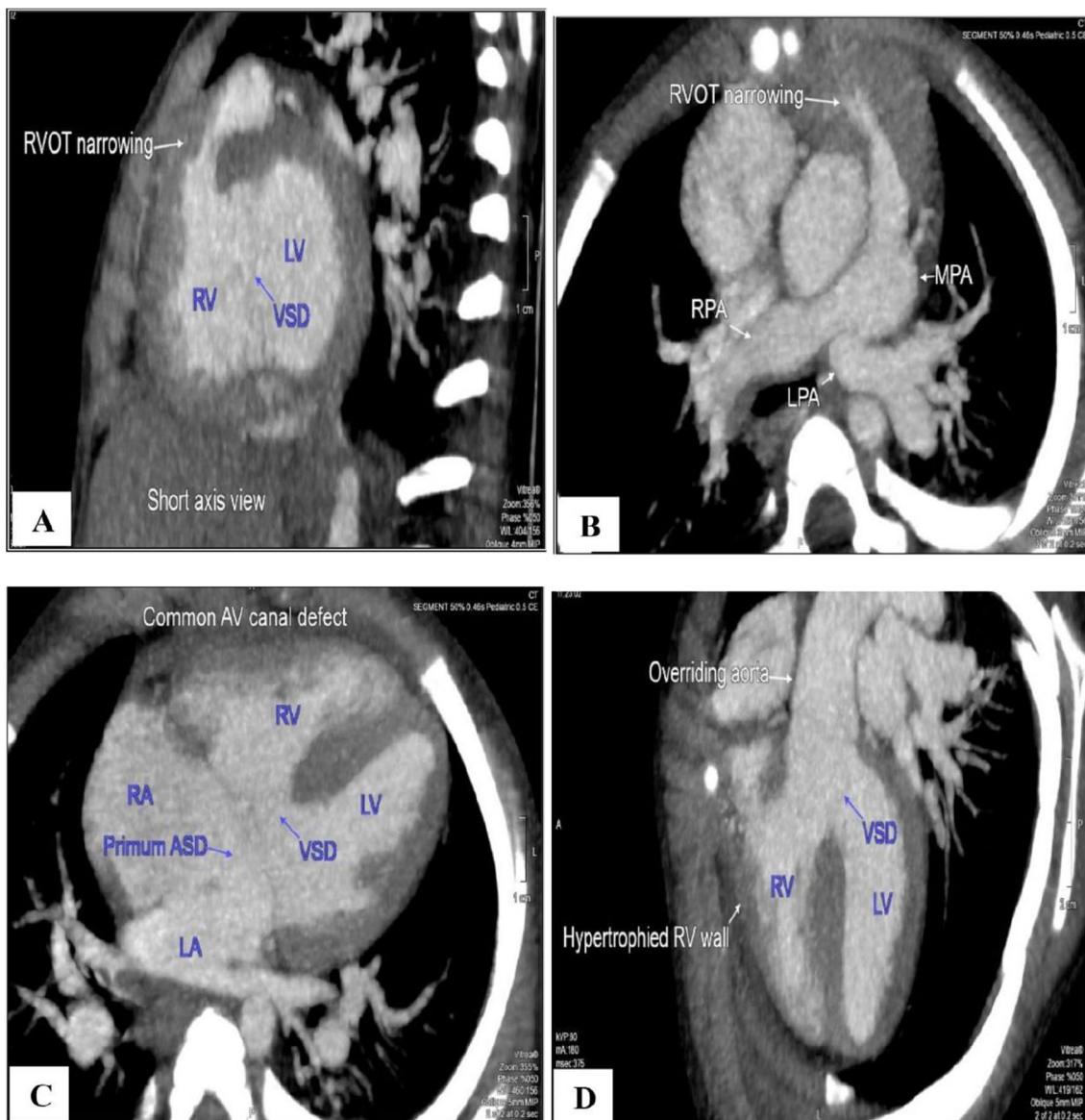


Fig. 3 12 months age down girl with Fallot’s tetralogy with common AV canal defect variant presented with tachypnea and irritability **A** Short axis view showing RVOT infundibular narrowing and large VSD. **B** Axial MIP image shows RVOT narrowing, valvular pulmonary stenosis and post stenotic dilatation of MPA. **C** Oblique 4-Chamber view showing ostium primum ASD, common AV canal defect including common atrioventricular valve and inlet VSD. **D** Oblique reformatted image showing overriding aorta, peri-membranous VSD and hypertrophies RV wall. **E, F** reformatted images showing average right and left pulmonary arteries with no focal stenosis. **G, H** VR images showing overriding aorta, RVOT narrowing, valvular pulmonary stenosis with post stenotic MPA dilatation. **I** VR image (posterior view) shows aberrant right subclavian artery. Note normal pulmonary venous drainage into the left atrium. **J** VR image of right ventricular outflow (RVOT) and pulmonary arterial tree shows RVOT narrowing, valvular pulmonary stenosis and post stenotic dilatation of MPA

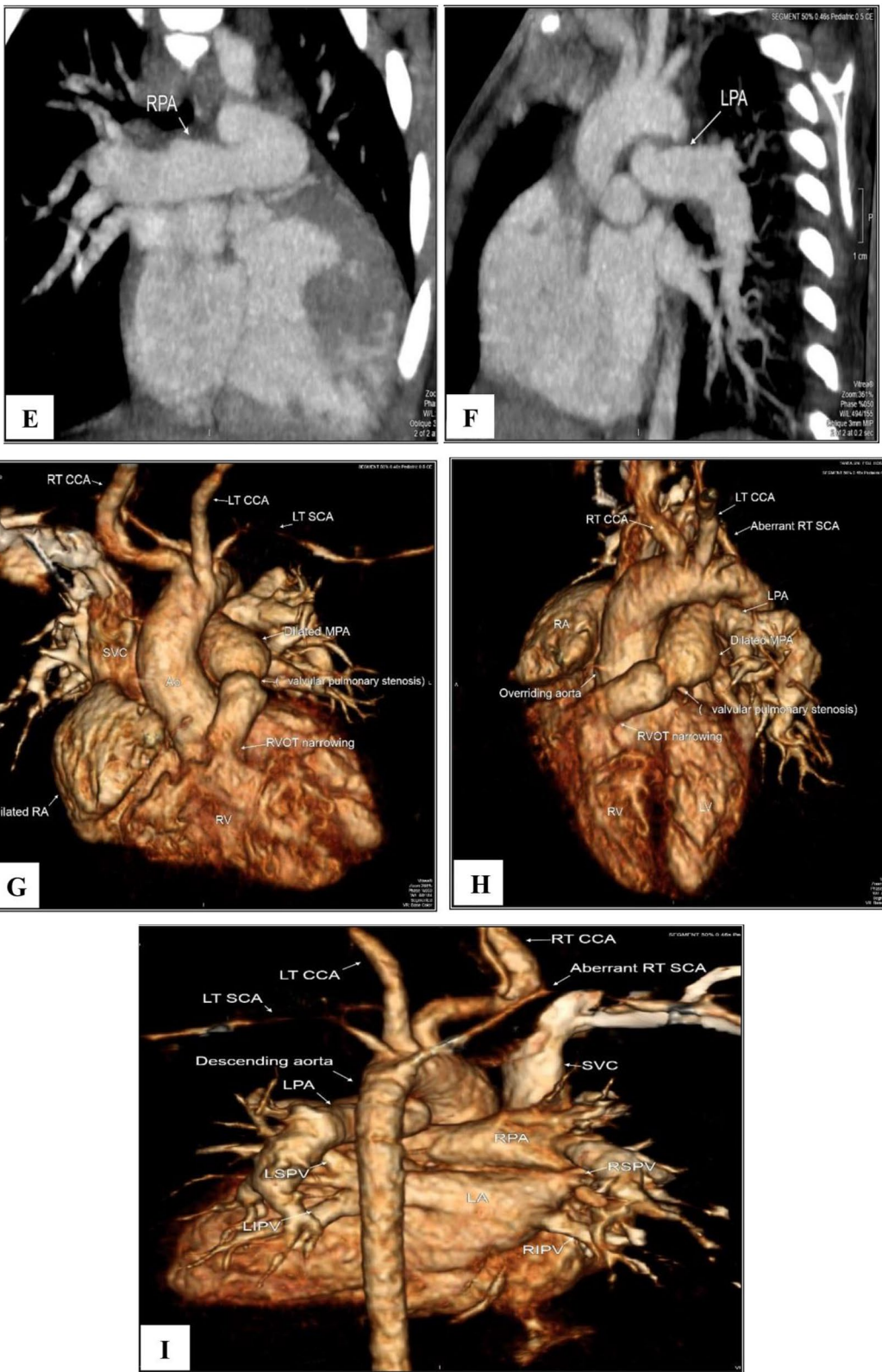


Fig. 3 continued

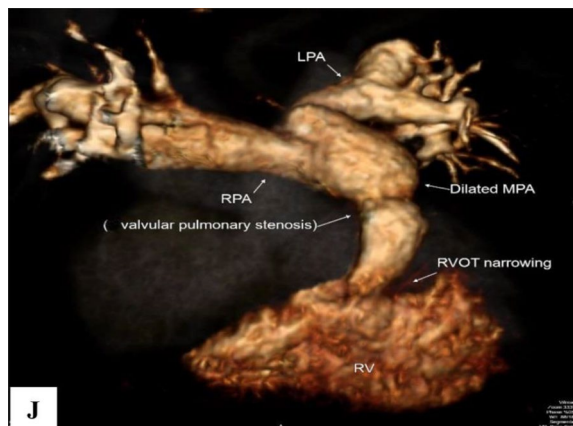


Fig. 3 continued

Mc-Nemar test showed statistically significant difference between both Echocardiography and MDCT in detecting supravalvular RVOTO at main pulmonary artery, right pulmonary artery and left pulmonary artery levels with P value 0.016, 0.008 and 0.008 respectively however non statistically significant difference was found between both in detection of sub-valvular and valvular level of RVOTO, the above findings were listed in Table 1.

Combined sub-valvular, valvular, and supravalvular pulmonary stenosis was the most common type of RVOTO that detected in 20 patients (40%), followed by isolated sub-valvular stenosis in 10 patients (20%). Combined sub-valvular and valvular stenosis was found in 7 patients (14%), however combined sub-valvular and supravalvular found in 8 patients (16%).

Degree of aortic overriding to the interventricular septum was assessed by MDCT and reported to be either equal alignment to both ventricles (50%), more to left ventricle alignment or more to right ventricle alignment. Equal alignment (50%) of the aorta to both ventricles was found in 33 patients (66%), more than 50% alignment to the left ventricle was found in 10 patients (20%) and 7 patients (14%) showed more than 50% alignment to the right ventricle.

Assessment of pulmonary circulation

Pulmonary arteries

Regarding MPA, MDCT detected pulmonary atresia in 14 patients representing 28% (13 patients showing atresia with confluent pulmonary arteries and one with absence of confluent pulmonary arteries). Echocardiography also diagnosed 14 patients (28%) with main pulmonary atresia, however it missed the presence of confluent pulmonary arteries in 3 patients and reported 10 patients as

atresia with confluent pulmonary arteries and four with absence of confluent pulmonary arteries.

MDCT detected focal main pulmonary artery stenosis in 6 (12%) patients; 4 cases (8%) just above the valve (supravalvular) and 2 (4%) showed distal MPA stenosis, while Echocardiography failed to detect them. MDCT also reported 10 patients (20%) with hypoplastic MPA versus 9 patients (18%) reported by Echocardiography. Dilated MPA was found in one patient showed post-stenotic dilatation by MDCT and missed by Echocardiography.

Regarding right pulmonary artery abnormalities MDCT revealed hypoplastic RPA in 12 patients (24%), ostial stenosis in 4 patients (8%), both hypoplasia and ostial stenosis in one patient (2%) and atretic RPA in one patient (2%). However, Echocardiography reported hypoplastic RPA only in 8 patients (16%), failed to diagnose four patients of attenuated caliber, four patients with ostial stenosis and one patient with combined RPA hypoplasia with ostial stenosis. Also, missed diagnosis of hypoplastic RPA in one patient.

MDCT could depict hypoplastic LPA in 13 patients (26%) compared to 8 patients (16%) reported by Echocardiography, ostial stenosis in 2 patients (4%), both hypoplasia and ostial stenosis in 2 patients (4%) and atretic LPA in one patient (2%). Echocardiography missed detection of ostial stenosis in two patients, combined hypoplasia with ostial stenosis in other two cases and one case of hypoplastic LPA.

Marginal Homogeneity test revealed statistically significant difference between both Echo, and MD CT in assessment of main, right and left Pulmonary arteries with P value = 0.036, 0.014 and 0.023 respectively as listed in Table 2.

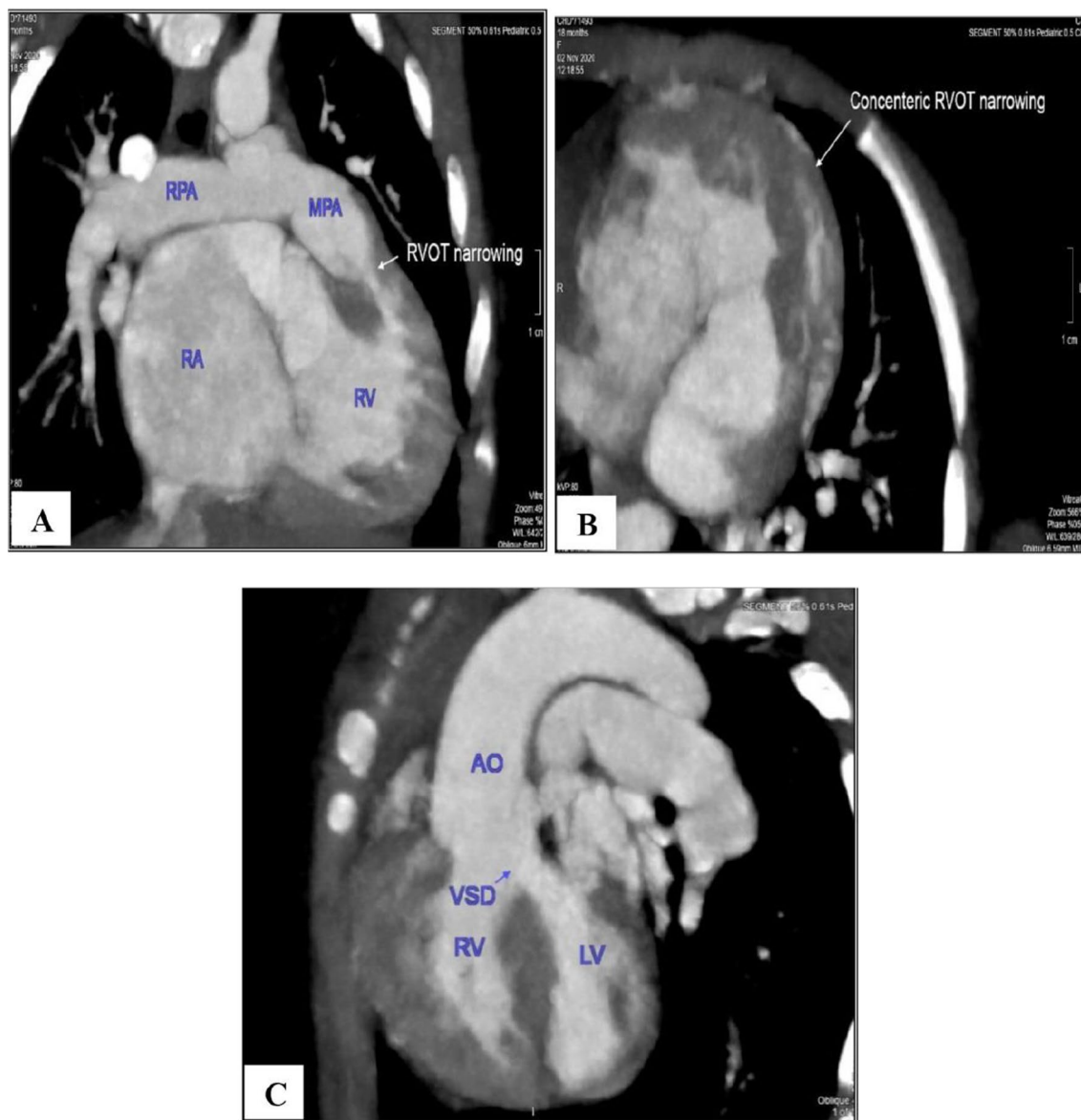


Fig. 4 18 months age girl with TOF DORV variant with clinical history of cyanosis and irritability. **A** MPR sagittal image showing infundibular RVOT stenosis with average MPA and RPA. **B** Axial MIP image showing concentric RVOT luminal narrowing. **C** Oblique reformatted image showing overriding aorta with ventricular septal defect (VSD) with more alignment of aorta to the right ventricle. **D, E** Axial MIP and MPR sagittal images showing PDA connected to LPA. **F, G** Axial and coronal MIP images showing superior sinus venosus ASD. Note Right superior and inferior pulmonary veins abnormal drainage by common ostium into the right sided atrium representing partial anomalous pulmonary venous connection. **H–J** Coronal MinIP image, Axial MIP and coronal MIP images showing left isomerism evident by bilateral left bronchial morphology (hypoarterial bronchus) (**G**), left sided polysplenia (**H**) as well as azygous continuation of IVC (**J**). **K** VR image anterior view showing MPA, RV, RA, ascending aorta and aortic arch with its branches. Note left atrial appendage morphology of the right atrial appendage. **L** VR image of the aorta and pulmonary arterial tree showing average sized MPA, RPA and LPA with PDA seen Connecting to LPA. **M, N** VR images posterior view showing abnormal drainage of right superior and inferior pulmonary veins by common ostium into the right sided atrium (partial anomalous pulmonary venous return) as well as azygous continuation of IVC. Note PDA arising from the inferior aspect of aortic arch

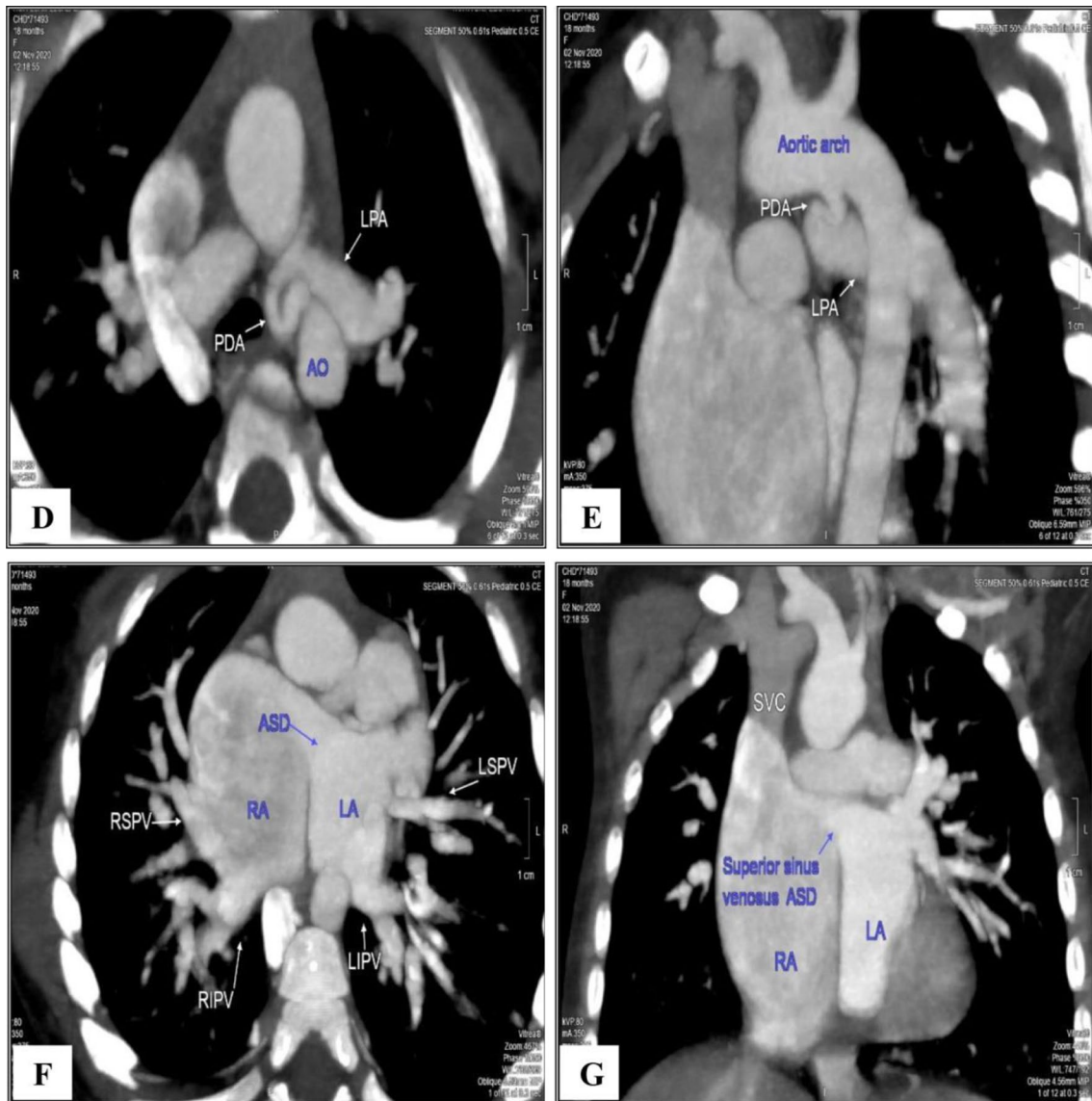


Fig. 4 continued

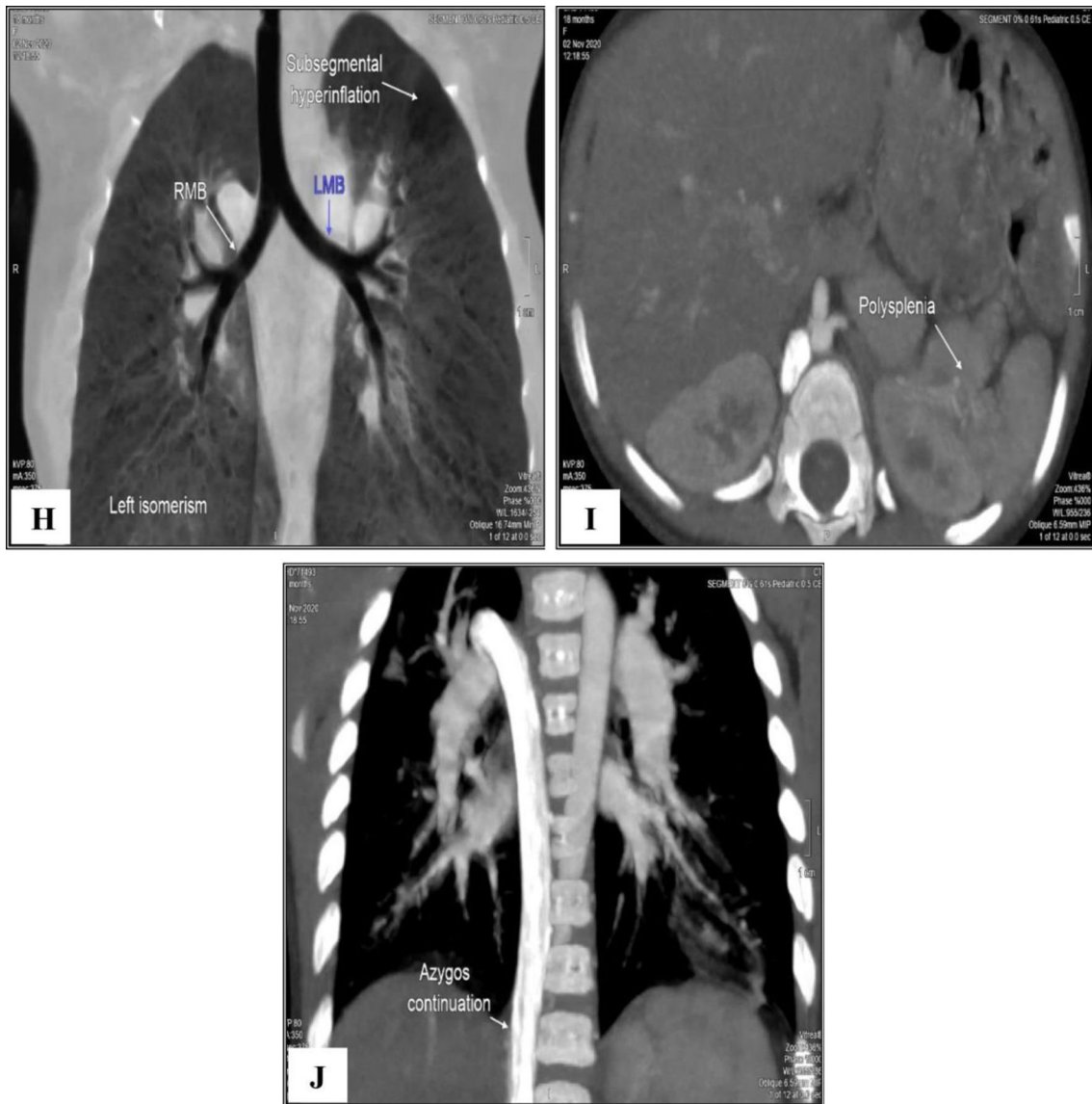


Fig. 4 continued

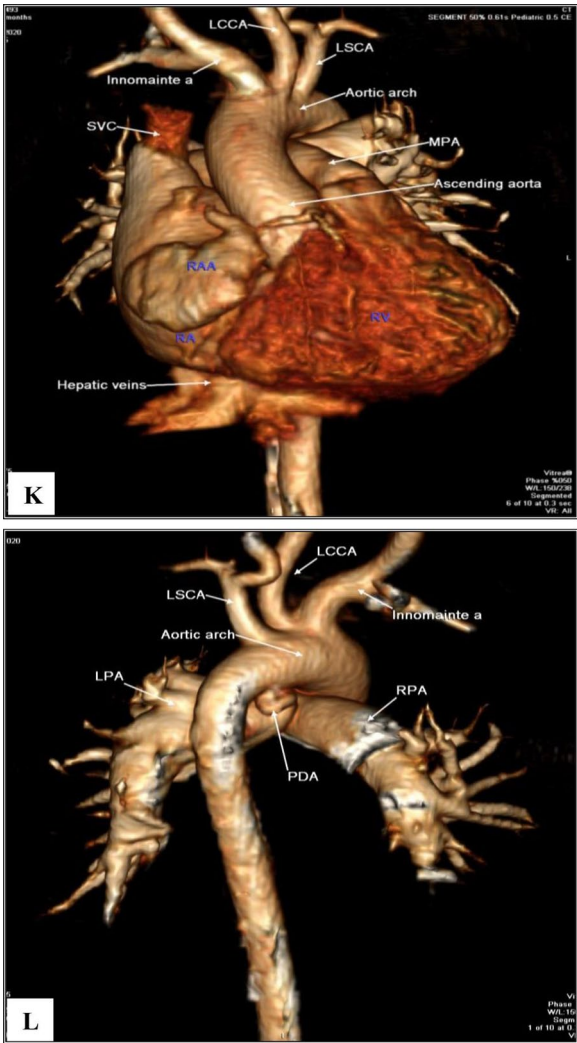


Fig. 4 continued

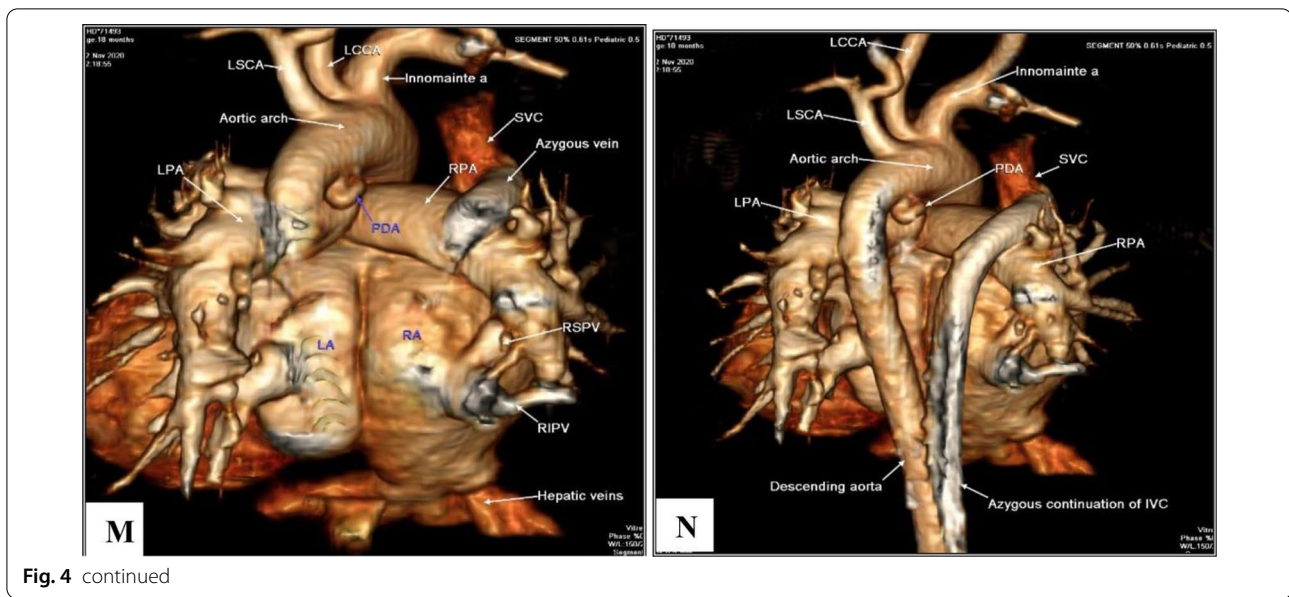


Fig. 4 continued

Table 1 Level of RVOTO in 50 studied cases

Level of RVOTO	ECHO		CT		McNemar test P value	Agreement	
	N	%	N	%		k	%
Sub-valvular (Infundibulum)	47	94.00	47	94.00	1.000	1.000	100
Valvular (stenosis/atresia)							
Valve stenosis	16	32.00	12	24.00	0.125	0.803	92
Valve atretic	18	36.00	18	36.00	1.000	1.000	100
Supravalvular (stenosis/hypoplasia/atresia)							
Main pulmonary artery	23	46.00	30	60.00	0.016*	0.724	86
Right pulmonary artery	10	20.00	18	36.00	0.008*	0.576	84
Left pulmonary artery	10	20.00	18	36.00	0.008*	0.576	84

P: P value for comparing between ECHO and MSCT. *Statistically significant at $P \leq 0.05$ k: Kappa test

Mc-Goon's ratio

CT Mc-Goon ratio was calculated to evaluate the size of pulmonary artery branches by measuring the summation of right and left pulmonary artery diameter at the point before its branching, divided by the diameter of the descending aorta at the level of the diaphragm [13]. Mc-Goon's ratio was calculated in all patients ($n=50$ cases). Out of 50 cases, Mc-Goon's ratio was favorable in 33 patients (66%), so this group of patients were adequate for complete surgical repair.

Pulmonary aortic connections

The cases examined for aorto-pulmonary connections were subclassified into patent ductus arteriosus (PDA) and major aorto-pulmonary collateral arteries (MAPCAs). These findings were correlated with the ability

of Echo to delineate them as a preoperative evaluation technique.

MDCT entailed 19 patients (38%) with PDA. Only 15 patients (30%) were depicted by Echocardiographic examination. MDCT detected PDA stenosis in 5 patients, 3 patients have narrowed pulmonary end while 2 patients had stenosed and obliterated aortic end. Chi square test revealed no statistically significant difference between both Echo, and MDCT in PDA ($P=0.527$).

Regarding MAPCAs, out of our 50 patients MDCT depicted 11 patients (22%) having MAPCAs with total number of MAPCAs=25 (3 patients had 1 MAPCA, 2 patients had 2 MAPCAs and 6 patients had 3 MAPCAs) however, Echocardiography detected only 7 patients (14%) with total number of MAPCAs=8. In addition, MDCT could detect stenosis in two MAPCAs. MDCT

Table 2 MPA, RPA and LPA abnormalities detected by Echo and MDCT in the studied cases ($n = 50$)

	ECHO		CT		Marginal homogeneity test	
	N	%	N	%	MH	P-value
MPA						
Normal	27	54.00	19	38.00	2.092	0.036*
Hypoplastic	9	18.00	10	20.00		
Supra-valvular stenosis	0	0.00	4	8.00		
Distal stenosis	0	0.00	2	4.00		
Atresia with confluent pulmonary arteries	10	20.00	13	26.00		
Atresia with non-confluent pulmonary arteries	4	8.00	1	2.00		
Dilated	0	0.00	1	2.00		
RPA						
Normal	40	80.00	32	64.00	2.462	0.014*
Hypoplastic	8	16.00	12	24.00		
Atresia	2	4.00	1	2.00		
Ostial stenosis	0	0.00	4	8.00		
Hypoplastic and ostial stenosis	0	0.00	1	2.00		
LPA						
Normal	40	80.00	32	64.00	2.278	0.023*
Hypoplastic	8	16.00	13	26.00		
Atresia	2	4.00	1	2.00		
Ostial stenosis	0	0.00	2	4.00		
Hypoplastic and ostial stenosis	0	0.00	2	4.00		

*Statistically significant at $P \leq 0.05$ **Table 3** ECHO and MDCT of Associated extracardiac vascular anomalies

Extracardiac vascular anomalies		ECHO		CT		Chi-square	
		N	%	N	%	χ^2	P-value
Aortic anomalies	Abnormal branching	4	8.00	24	48.00	17.907	<0.001*
	<i>Bovine</i>	0	0.00	7	14.00	5.530	0.019*
	<i>Left vertebral artery from arch</i>	0	0.00	5	10.00	3.368	0.067
	<i>Aberrant right subclavian a</i>	0	0.00	2	4.00	0.510	0.475
	<i>Mirror imaging branching</i>	4	8.00	10	20.00	2.076	0.150
	Side	4	8.00	10	20.00	2.076	0.150
	Right sided arch						
	Aortic coarctation	1	2.00	2	4.00	0.000	1.000
Prominent bronchial vessel		0	0.00	2	4.00	0.510	0.475
PAPVR		0	0.00	1	2.00	0.000	1.000
TAPVR		0	0.00	1	2.00	0.000	1.000
Azygous continuation of IVC		0	0.00	1	2.00	0.000	1.000

*Statistically significant at $P \leq 0.05$

could also evaluate the origin, size and course of these MAPCAs as well as lung segments supplied by them.

Pulmonary veins

Pulmonary venous abnormalities were detected by MDCT in 2 patients (4%), one had partial anomalous

pulmonary venous return (PAPVR) and the other had supra-cardiac total anomalous pulmonary venous return (TAPVR). Echocardiography missed the diagnosis of both of them. MDCT described the detailed anatomy of the vertical vein and the site of its drainage in patient with TAPVR.

Assessment of ascending aorta and arch of aorta

Clockwise rotation of aortic root was depicted in all patients. 38 patients (76%) showed dilated ascending aorta. 10 patients (20%) had right sided aortic arch and 40 (80%) had left sided arch. Regarding branching pattern of aortic arch, MDCT depicted normal branching pattern in 26 patients (52%) while the 24 patients (48%) showed abnormal branching pattern; mirror image branching pattern in 10 patients (20%), bovine aortic arch with common origin of right innominate and left common carotid artery in 7 patients (14%), left vertebral artery origin from aorta in 5 patients (10%) and aberrant right subclavian artery in 2 patients (4%). MDCT detected aortic coarctation in two patients (4%) and bicuspid aortic valve in another patient (2%).

Coronary arteries assessment

By MDCT assessment, eight patients (16%) had coronary arteries abnormalities that were of value in preoperative assessment of TOF patients. 6 patients (12%) had prominent RV/conus branches. One patient (2%) had dual LAD with additional one arising from the RCA and other patient had anomalous origin of LAD from RCA. Echocardiography depicted only three of the prominent RV/conus branches and missed detection of Dual LAD and anomalous origin of LAD in other two patients. Chi-square test revealed no statistically significant difference between Echo, and MDCT in detection of coronary anomalies ($P=0.350$).

Associated intracardiac anomalies

25 patients (50%) had ASD; 10 patients (20%) had ostium secundum ASD, 11 (22%) had patent foramen ovale, 3 (6%) had ostium primum ASD and 1 patient (2%) had superior sinus venosus ASD. MDCT examination missed detection of ostium secundum ASD in 2 patients and patent foramen ovale in other 2, while Echocardiography misdiagnosed superior sinus venosus ASD that was depicted by MDCT in 1 patient. MDCT detected additional muscular VSD in 4 patients (8%) versus 3 (6%) reported by Echocardiography. Chi square test revealed no statistically significant difference between both Echo, and MDCT in detection of associated intracardiac defects as well as chambers abnormality. MDCT and Echocardiography diagnosed abnormalities of cardiac chambers accurately with the most common chamber abnormality detected in this study was dilated right side cardiac chambers founded in 28 patients (56%) with 100% agreement between the two imaging modalities.

Associated extracardiac vascular anomalies

As regard associated aortic anomalies, Echocardiography missed diagnosis of 6\10 patients of right sided aortic arch. It also missed detection of bovine arch in 7 patients, left vertebral artery from the aortic arch in five patients and aberrant right subclavian artery in 2 patients. These findings were correctly depicted by MDCT. MDCT reported two patients with aortic coarctation however Echocardiography missed one of them. MDCT examination reported two patients with prominent bronchial vessels, one patient with partial anomalous pulmonary venous return, one patient with total anomalous pulmonary venous return of supra-cardiac type and one patient with interrupted inferior vena cava (IVC) with azygous continuation, these findings missed by Echocardiography. Chi square test revealed a statistically significant difference between both Echo, and MDCT in detection of associated aortic lesions ($P<0.001$). No statistically significant difference on other detected lesions, the above findings were listed in Table 3.

40 patients (80%) were operated and 10 patients (20%) only performed catheterization. We compared the Echo and MDCT findings with the data collected by cardiac catheterization and/or operation. MDCT could correctly depict all aortic, coronary and other associated extracardiac vascular anomalies including pulmonary aortic connections (PDA and MAPCAs) by axial, multiplanar and three-dimensional images with 100% sensitivity and 100% specificity.

Extra-cardiac non-vascular findings

In this study, 15 patients (30%) showed patches of pulmonary consolidation, 2 patients (4%) had hyperinflated lung segments, one patient (2%) showed bilateral bilobed lung morphology in a case of left isomerism, bronchus suis in one patient (2%), abnormal bronchial branching pattern of bilateral hyperarterial morphology in one patient (2%) of left isomerism, dorsal hemi-vertebras in one patient (2%), partial fused of ribs in 1 patient (2%) and short rib in other one (2%), left sided polysplenia in 1 patient (2%) and absent kidney in another one (2%).

Radiation dose

The effective radiation dose in milli-Sievert was calculated by multiplying the DLP (automatically estimated by CT scanner) by conversion coefficient factor that differs according to age. The mean absorbed radiation dose of the 50 scans was 72.066 ± 14.048 mGy-cm per scan and the mean effective dose was 1.960 ± 0.657 mSv.

Discussion

In the current era, TOF is almost universally amenable to surgical repair with good long-term outcome. This, however, requires a thorough pre-operative anatomic description of central and branch pulmonary arteries and associated defects, like additional muscular VSD, ductus arteriosus (PDA), Major Aortopulmonary Collateral Arteries (MAPCAs) [14].

MSCT, including CT angiography (CTA), provides an important diagnostic tool for evaluation patient with CHD even in small infants with its high scanning speed, superior spatial resolution and improved capabilities for concurrent assessment of cardiovascular structures and lung parenchyma. It can provide accurate three-dimensional depictions of complex cardiac morphology of TOF and extra-cardiac association, tracheobronchial tree and pulmonary parenchymal assessment. It can also permit evaluation of associated coronary artery anomalies and aorto-pulmonary collateral vessels [15, 16].

320-MDCT system allows axial volumetric scanning with 160 mm of coverage in the z direction as the detector element consists of 320×0.5 mm detector permitting imaging the heart in a single 0.35-s gantry rotation without table movement. It offers advantages of decreased motion artifacts, reduced scan durations and need for sedation. It also reduced contrast agent volume requirements as well as patient radiation exposure due to lack of z-axis overranging and overlapping helical rotations in addition to minimal penumbral overbeaming with volumetric scanning. It allows excellent anatomic imaging of the whole heart, great vessels and the coronaries [17].

Retrospective ECG gating with a 320-slice scanner utilizing low dose protocol was performed in all cases complying with ALARA (As Low As Reasonably Achievable) principle, in the form of reduction of Kvp and automatic adjustment of tube current according to body weight. Low radiation dose protocol of 80 kV in 48 patients and 100 kV in 2 older patients with automatic adaptation of the mAs. The average dose length product was 72.066 ± 14.048 mGy-cm and the effective radiation dose was 1.960 ± 0.657 mSv.

This was significantly lower than study by Singh et al. [18] and Lin et al. [19] who used 64 MDCT in their studies with adapting dose parameters to body habitus and dose saving strategies with the mean of the effective dose reduction was 4.5 mSv and dose length product 115–218 mGy cm This may be attributed to the advantage of volumetric scanning over helical scanning in reducing the time of scanning and the radiation dose. However Al-Mousily et al. [20], who used prospective cardiac gating on a 320-slice CT, their study reported more dose reduction to 0.8 ± 0.39 mSv and it is owing to

use of prospective ECG gating which has the advantage of markedly reduced radiation exposure as the patient is irradiated only at selectable heart phases than the radiation used in our study in retrospective ECG gating.

This study included 22 patients with classic TOF (TOF/PS), 18 patients with TOF pulmonary atresia (PA/VSD) variant, 3 patients with TOF CAVC variant and 7 patients with TOF DORV variant.

According to the status of native pulmonary arteries, MAPCAs and PDA, PA-VSD is classified to Type A where native pulmonary arteries are present and the pulmonary vascular supply through PDA (no MAPCAs), Type B where native pulmonary arteries and MAPCAs are present and Type C with no native pulmonary arteries and the pulmonary supply through MAPCAs only [21]. Out of the 18 patients of PA-VSD variant. 12 patients were of type A, 5 were of type B and only one case was of type C.

Abnormal situs is a rare finding in TOF patients as mentioned by Zakaria et al. [22]. We encountered only one case situs ambiguous (left isomerism). This finding was only depicted by MDCT and had not been detected in echocardiography. This could be attributed to the superior role of cross-sectional imaging in cardiac, bronchial and abdominal viscera evaluation that help in situs determination.

Regarding TOF cardinal features; with evaluation of interventricular communication outlet subaortic perimembranous cono-truncal VSDs found in 47 patients (94%). 3 cases showed large inlet VSD extending to the outlet region seen in the TOF CAVC variant. Identifying presence of additional muscular VSD is such an important issue as additional VSD must be closed during surgical repair to avoid pulmonary over flow after surgical correction [3]. In our study 4 patients had additional muscular VSD detected by MDCT, Echocardiography missed one of them and detected only 3. This matches with explanation of Shaaban et al. [3] in their study that these VSD usually require special attention as they may be sometimes difficult to identify by echocardiography because the large cono-truncal VSD equalizes LV and RV pressures making no significant pressure gradient across these additional VSDs. However, Moustafa et al. [5] in their study detected additional muscular VSD in 4 cases using MDCT opposite 5 cases by echocardiography attributing their finding to the to the ability of color Doppler to detect very small intermuscular defect rather than MDCT.

Regarding right ventricular hypertrophy (RVH), we noted that all cases showed RVH by MDCT matching with Moustafa et al. [5] in their study.

Assessment of degree of aortic overriding is important for surgical planning of VSD patch closure as patients

with DORV will need much larger patch to baffle the blood from the left ventricle to the aortic root [23]. In our study we reported equal alignment of the aorta to both ventricles in 33 patients (66%) representing the most frequent alignment, more than 50% alignment to the left ventricle was found in 10 (20%) patients. 7 patients (14%) showed more than 50% alignment to the right ventricle in TOF/DORV variant. Our results were matching with what Moustafa et al. [5] reported in their study where equal aortic overriding was the most encountered and found in (60/77 patients representing 78% however followed by more from the RV in 15 patients (19.5%) then more to the LV alignment only in 2 patients (2.6%) in contrast to our findings where left ventricular alignment was encountered in more cases than right ventricular alignment.

With studying level of obstruction in every patient, 47 patients had sub-valvular pulmonary stenosis representing the most commonly affected level. This came in agreement with what Hrusca et al. [1] stated in their study where they studied pulmonary artery anomalies in tetralogy of Fallot using non-ECG-gated CT angiography and found that 24 patients (68.57%) had infundibular stenosis. Also, Singh et al. [18] as well as Moustafa et al. [5] reported in their recent studies that sub-valvular (infundibular) stenosis was the most commonly affected level of their patients.

We also found that combined level of obstruction was much more common than isolated level of obstruction with combined sub-valvular, valvular, and supra-valvular stenosis was detected in 40% of patients matching with Moustafa et al. [5] findings in their study. In the study performed by Singh et al. [18], it was encountered that infundibular with valvular stenosis was the most common type of RVOT obstruction (47.28%) followed by isolated infundibular stenosis.

In our study MDCT and Echocardiography showed 100% agreement in detection of sub-valvular stenosis as well as valve atresia however MDCT missed diagnosis of valve stenosis in four patients compared to Echocardiography. Less agreement with statistically significant difference between the two modalities in detecting the supra-valvular stenosis where echocardiography missed detection of supra-valvular RVOTO in MPA, RPA and LPA levels. These findings came in agreement with Hu et al. [24] who reported 100% accuracy of MDCT in detection of supra-valvular pulmonary stenosis comparing their result to cardiac catheterization.

Regarding pulmonary arteries characterization, a statistically significant difference was found between both Echo, and MDCT in assessment of main, right and left pulmonary arteries. MDCT could efficiently detect supra-valvular and distal stenosis in main pulmonary

artery as well as ostial stenosis in their branches while echocardiography failed to detect them. Also, Echocardiography failed to detect hypoplastic main and branch pulmonary arteries in other cases as well as missed depiction of confluent hypoplastic branch pulmonary arteries and reported them as atretic. Apostolopoulou et al. [25] in their study recommended MDCT in evaluation of complex pulmonary artery defects in TOF patients for better visualization pulmonary arteries anatomy, size, and arborization matching with our results. Raimondi et al. [26] as well stated in their study the role of CT scans in definition the distal anatomy of pulmonary branches.

In the current study level of obstruction at MPA (stenosis, hypoplasia or atresia) was found in 30(60%) patients followed by RPA and LPA with 18 (36%) patients for each. These findings came in agreement with Moustafa et al. [5] and Zakaria et al. [22] who reported incidence of combined MPA stenosis and its branches 17% as the most common pulmonary artery anomaly. While it disagrees with Sheikh et al. [14] who stated that isolated left pulmonary stenosis was the most common abnormality in 10%. This was attributed by Moustafa et al. [5] to larger number of patients (about 5000) included in the study who underwent cardiac catheterization.

Mc-Goon's ratio is an applicable method to evaluate the pulmonary arterial size and pulmonary blood flow. When the Mc-Goon ratio is adequate, it means enough pulmonary blood, and hence total surgical correction is planned. Otherwise, palliative operation is suggested in case of inadequate Mc-Goon's ratio [27]. In our study, 33 patients had ratio more than 1.2. This group are candidate for total repair. Chen et al. [27] who stated that MDCT with reconstructed oblique images are reliable methods for Mc-Goon ratio calculation when they compared it to the angiographic findings.

In this study MSCT entailed 19 patients with PDA versus 15 patients depicted by echocardiography. CT could also detect tight PDA pulmonary end in three patients, stenosed and obliterated aortic end in other two. However, echocardiography failed to detect them. This coincides with Moustafa et al. [5] and Shehata et al. [28] studies. They stated the superior role MDCT over transthoracic echocardiography in evaluation of PDA. Ishihara et al. [29] in their study also recommended MSCT for better evaluation of doubtful cases of PDA with normal echocardiography. However, Leschka et al. [30] in their study reported TTE as the method of choice for diagnosing PDA while MDCT has only a minor role. Regarding MAPCAs, MSCT had depicted 25 MAPCAs per 11 patients representing a percentage of 22%. Juneja et al. [31] in their study documented an incidence of 56% of MAPCAs in TOF patients. Their study included homogenous group of TOF patients with pulmonary

atresia, however our study included different TOF variants with different pulmonary defects.

Echocardiography only detected 8 MAPCAs per 7 patients. In addition, CT detected stenosis in MAPCA in two patients besides its role in evaluation the origin, numbers, size and course and lung segments supplied by these MAPCAs, which agreed with study did by Hu et al. [24], they stated the superior role of CT in evaluation of number, origin, and supplied lung lobes of MAPCAs regardless of the size however TTE can only identify relatively large ones. Also Chandrashekhar et al. [32] stated that MDCT had the ability similar to catheterization in aortopulmonary collateral identification, while it is difficult to detect these collaterals by echocardiography mainly secondary to small field of view.

Being aware of anomalous pulmonary venous return in TOF patients prior to surgical correction is an important issue to avoid catastrophic outcomes [33]. In our study TAPVR of supracardiac type was identified in one patient and PAPVR in another one with MDCT while missed by echocardiography matching with Türkvan et al. [34], they stated more reliability of MDCT than TTE in delineation of the PAPVR. Chan et al. [35] in their study concluded that repaired TOF patients with unrepaired PAPVR were liable to more RV volume overload and more reduction in RV function.

Lack of conal rotation and conal malseptation is a characteristic anatomical feature of TOF which lead to dextroposed position of the aorta and significant RVOT narrowing [36]. In this study, with thorough assessment of ascending aorta and aortic root by MDCT, Clock wise rotation (dextroposition) of aortic root was encountered in all patients. In addition, 38 patients showed dilated ascending aorta representing 76%.

In spite of the absence of functional significance of the right sided arch, it is important to tell surgeons beforehand to avoid complications [14].

In our study right sided aortic arch was found in 10 patients with percentage of 20%. This was comparable to documented incidence of 20–25% cases by Kemper et al. [37] and Siripornpitak et al. [38].

Regarding branching pattern of aortic arch, MDCT depicted normal branching pattern in 26 patients while the other 24 patients showed abnormal branching pattern; mirror image branching pattern in 10 patients, bovine aortic arch with common origin of right innominate and left common carotid artery in 7 patients, left vertebral artery origin from aorta in 5 patients and aberrant right subclavian artery in 2 patients. In addition, MDCT detected aortic coarctation in 2 patients and bicuspid aortic valve in another patient.

Preoperative assessment of coronary artery anomalies is essential for patients with TOF to avoid injury

of aberrant coronary artery passing across the RVOT in ventriculotomy or trans annular repair when done to relieve the RVOT [24]. Although Echocardiographic analysis remains the first step in the evaluation of patients with congenital heart defects, it might be limited to depict anomalous coronary arteries in patients with TOF [39].

In our study coronary artery abnormalities were identified in 8 patients with percentage of 16%. MDCT detected one patient with dual LAD where another LAD seen originating from RCA. Another patient showed anomalous origin of LAD from RCA. Echocardiography failed to detect both of them. 6 patients depicted by CT having prominent conus/RV branches. Echocardiography missed three of them. These findings were in accordance with Amzallag el al. [39] in their study wherein 3 of 7 cases, an anomalous coronary artery were missed by means of echocardiographic analysis. Superiority of MDCT in detection of coronary artery anomalies compared to Echocardiography coincides Moustafa et al. [5] as well as Shehata et al. [28] and Gotein et al. [10]. Also Hu et al. [24] in their study described the coronary artery anomalies at 2 cases with sensitivity 100% and specificity 100% when compared to cardiac catheterization.

There is a high incidence of associated extracardiac vascular anomalies in pediatric patients with TOF, and these abnormalities might preclude certain types of surgical repair and may provoke late adverse outcomes [24, 40].

As regard to associated extra cardiac vascular anomalies, Echocardiography missed detection of 6 patients with right sided aortic arch out of 10 depicted by MDCT examination. It also failed in detection of bovine aortic arch, left vertebral artery origin from the aorta and aberrant right subclavian artery in other 14 patients. These results came in line with Eltatawy et al. [41] in their study where they confirmed the efficacy of MDCT in identifying different aortic arch branching pattern. This could be attributed to the small field of view during examination from the suprasternal direction could be the main reason why the great vessels could not be identified as accurately using TTE. Moreover, the short neck of pediatric patients, the overlying bone, and the aerated lung might also influence the diagnostic value of TTE in the depiction of these deformities.

Comparing MDCT findings with the data collected by cardiac catheterization and/or operation, MDCT could correctly depict all aortic, coronary and other associated extracardiac vascular anomalies including pulmonary aortic connections (PDA and MAPCAs) by axial, multiplanar and three-dimensional images with 100% sensitivity and 100% specificity.

These findings came in agreement with Hu et al. [24] they stated the superiority of MDCT over TTE in detecting extracardiac vascular anomalies in pediatric patients with complex CHD such as TOF.

A major limitation in this study was the relatively small number of the studied cases that rendered giving a full idea about the diagnostic efficacy of cardiac MDCT. Retrospective ECG gating was another limitation that relatively increase the radiation dose in infants and children. However, with performing low dose protocol in all cases complying with ALARA principle radiation exposure was minimized as much as possible.

We recommended careful selection of TOF patients for cardiac MDCT imaging and application of strategies for radiation exposure reduction. We also recommend increasing the sample size in the future.

Conclusion

MDCT offers comprehensive anatomical assessment of TOF, and its variants providing superiority over echocardiography and comparable results to cardiac catheterization with 100% sensitivity and specificity in evaluation of associated extracardiac vascular anomalies as well as pulmonary arteries characterization.

It is worth using MDCT routinely in combination with echocardiography for the preoperative assessment of TOF and its variants representing a less invasive option than conventional catheterization with lower radiation exposure.

Abbreviations

ASD: Atrial septal defect; CAVC: Common atrioventricular canal; CPR: Curved planer reformations; DORV: Double-outlet right ventricle; IVC: Inferior vena cava; LPA: Left pulmonary artery; MAPCAs: Major Aortopulmonary Collateral Arteries; MDCT: Multidetector computed tomographic; MIP: Maximum intensity projections; MPA: Main pulmonary artery; MPR: Multiplanar reformations; MRA: Magnetic resonance angiography; PA: Pulmonary atresia; PAPVR: Partial anomalous pulmonary venous return; PDA: Patent ductus arteriosus; RPA: Right pulmonary artery; RVOTO: Right Ventricular Outflow Tract Obstruction; TAPVR: Total anomalous pulmonary venous return; TOF/PS: TOF with pulmonary stenosis; TOF: Tetralogy of Fallot; VR: Volume rendering; VSD: Ventricular septal defect.

Acknowledgements

To all the participants for their cooperation and patience.

Authors' contributions

MD suggested the research idea, ensured the original figures and data in the work, minimized the obstacles to the team of work, correlated the study concept and design and had the major role in analysis, EE collected data in all stages of manuscript, performed data analysis. MA and HZ supervised the study with significant contribution to design the methodology, manuscript revision and preparation. AB correlated the clinical data of patient and matched it with the findings, drafted and revised the work. All authors read and approved the final manuscript manuscript.

Funding

No funding. Not applicable for this section.

Availability of data and materials

The authors confirm that all data supporting the finding of the study are available within the article and the raw data and data supporting the findings were generated and available at the corresponding author on request.

Declarations

Ethics approval and consent to participate

Informed written consents taken from the patients and healthy volunteers, the study was approved by ethical committee of Tanta university hospital, faculty of medicine. Committee's reference number: 33357/09/19.

Consent for publication

All participants included in the research gave written consent to publish the data included in the study. Authors accepted to publish the paper.

Competing interests

The authors declare that they have no competing of interests.

Author details

¹Radiodiagnosis and Medical Imaging, Faculty of Medicine, Tanta University, El Gharbia, El-geish Street, Tanta, Gharbya Governorate, Egypt. ²Cardio-thoracic Surgery, Faculty of Medicine, Tanta University, El-geish Street, Tanta, Gharbya Governorate, Egypt.

Received: 27 October 2021 Accepted: 25 January 2022

Published online: 07 February 2022

References

- Hrusca A, Rachisan AL, Gach P et al (2016) Detection of pulmonary and coronary artery anomalies in tetralogy of Fallot using non-ECG-gated CT angiography. *Diagn Interv Imaging* 97:543–548. <https://doi.org/10.1016/j.diii.2016.03.010>
- Bedair R, Iriart X (2019) Educational series in congenital heart disease: tetralogy of Fallot: diagnosis to long-term follow up. *Echo Res Pract* 6:9–23. <https://doi.org/10.1530/ERP-18-0049>
- Shaaban M, Tantawy S, Elkafrawy F et al (2020) Multi-detector computed tomography in the assessment of tetralogy of Fallot patients: is it a must? *Egypt Heart J* 72:1–13
- Khatri S, Varma SK, Khatri P et al (2008) 64-Slice multidetector-row computed tomographic angiography for evaluating congenital heart disease. *Pediatr Cardiol* 29:755–762
- Moustafa S, Hussein MM, Sultan AA et al (2021) Three steps approach for preoperative evaluation of tetralogy of Fallot patients: role of 128 MDCT. *Egypt J Radiol Nucl Med* 52:1–14
- Bayraktutan U, Kantarci M, Ogul H et al (2013) The utility of multidetector computed tomography for evaluation of congenital heart disease. *Folia Morphol* 72:188–196. <https://doi.org/10.5603/FM.2013.0032>
- Anne MV, Stephen C, Pierluigi F et al (2014) Multimodality imaging guidelines for patients with repaired tetralogy of Fallot: a report from the American Society of Echocardiography: developed in collaboration with the Society for Cardiovascular Magnetic Resonance and the Society for Pediatric Radiology. *J Am Soc Echocardiogr* 27:111–141. <https://doi.org/10.1016/j.echo.2013.11.009>
- Frush DP (2009) Thoracic cardiovascular CT: technique and applications. *Pediatr Radiol* 39(464):470
- Thomas KE, Wang B (2008) Age-specific effective doses for pediatric MSCT examinations at a large children's hospital using DLP conversion coefficients: a simple estimation method. *Pediatr Radiol* 38:645–656. <https://doi.org/10.1007/s00247-008-0794-0>
- Goitein O, Salem Y, Jacobson J et al (2014) The role of cardiac computed tomography in infants with congenital heart disease. *Isr Med Assoc J* 16:147–152
- Einstein AJ, Moser KW, Thompson RC et al (2007) Radiation dose to patients from cardiac diagnostic imaging. *Circulation* 116:1290–1305. <https://doi.org/10.1161/CIRCULATIONAHA.107.688101>

12. Shrimpton PC, Jansen JTM, Harrison JD (2016) Updated estimates of typical effective doses for common CT examinations in the UK following the 2011 national review. *Br J Radiol* 89(1057):20150346. <https://doi.org/10.1259/bjr.20150346>
13. Sirichongkolthong B (2018) Correlation between aortic oxygen saturation and pulmonary artery size in cyanotic congenital heart disease with decreased pulmonary blood flow. *Ramathibodi Med J* 41:21–29. <https://doi.org/10.14456/rmj.2018.30>
14. Sheikh AM, Kazmi U, Syed NH (2014) Variations of pulmonary arteries and other associated defects in Tetralogy of Fallot. *Springerplus* 3:4–7
15. Haramati LB, Glickslein JS, Issenberg HJ (2002) MR imaging and CT of vascular anomalies and connections in patients with congenital heart disease: significance in surgical planning. *Radiographics* 22:337–349. <https://doi.org/10.1148/radiographics.22.2.g02mr09337>
16. Sarwar HO, Raza HO, Khurram N et al (2006) Assessment of cardiac function using multidetector row computed tomography. *J Comput Assist Tomogr* 30:555–563. <https://doi.org/10.1097/00004728-200607000-00001>
17. Podberesky DJ, Angel E, Yoshizumi TT, Toncheva G et al (2012) Radiation dose estimation for prospective and retrospective ECG-gated cardiac CT angiography in infants and small children using a 320-MDCT volume scanner. *Am J Roentgenol* 199:1129–1135. <https://doi.org/10.2214/AJR.12.8480>
18. Singh RKR, Jain N, Kumar S et al (2019) Multi-detector computed tomography angiographic evaluation of right ventricular outflow tract obstruction and other associated cardiovascular anomalies in tetralogy of Fallot patients. *Pol J Radiol* 84:511–516. <https://doi.org/10.5114/pjr.2019.91203>
19. Ming TL, Jou-Kou W, Yih-Sharn C et al (2011) Detection of pulmonary arterial morphology in tetralogy of Fallot with pulmonary atresia by computed tomography: 12 years of experience. *Eur J Pediatr* 171:579–586. <https://doi.org/10.1007/s00431-011-1621-4>
20. Faris AM, Roger YS, Frederick JF et al (2011) Use of 320-detector computed tomographic angiography for infants and young children with congenital heart disease. *Pediatr Cardiol* 32:426–432. <https://doi.org/10.1007/s00246-010-9873-8>
21. Duraisamy B, Muhammad D (2007) Pulmonary atresia with ventricular septal defect: systematic review. *Heart Views* 8:52–61
22. Zakaria RH, Barsoum NR, Asaad RE et al (2011) Tetralogy of Fallot: imaging of common and uncommon associations by multidetector CT. *Egypt J Radiol Nucl Med* 42:289–295. <https://doi.org/10.1016/j.ejrmn.2011.07.003>
23. Khan SM, Drury NE, Stickley J et al (2019) Tetralogy of Fallot: morphological variations and implications for surgical repair. *Eur J Cardiothorac Surg* 56:101–109. <https://doi.org/10.1093/ejcts/ezy474>
24. Hu B, Shi K, Deng Y-P et al (2017) Assessment of tetralogy of Fallot-associated congenital extracardiac vascular anomalies in pediatric patients using low-dose dual-source computed tomography. *BMC Cardiovasc Disord* 17:1–8
25. Apostolopoulou SC, Manginas A, Kelekis NL et al (2019) Cardiovascular imaging approach in pre and postoperative tetralogy of Fallot. *BMC Cardiovasc Disord* 19:1–12. <https://doi.org/10.1186/s12872-018-0996-9>
26. Raimondi F, Warin-Fresse K (2016) Computed tomography imaging in children with congenital heart disease: indications and radiation dose optimization. *Arch Cardiovasc Dis* 109:150–157. <https://doi.org/10.1016/j.acvd.2015.11.003>
27. Chen B-B, Chen S-J, Wu M et al (2007) EBCT-McGoon ratio a reliable and useful method to predict pulmonary blood flow non-invasively. *Medicine* 32:1–8. <https://doi.org/10.5114/amsad.2018.76824>
28. Shehata SM, Zaiton FM, Abo Warda MH et al (2017) Value of MDCT as a non-invasive modality in evaluation of pediatric congenital cardiovascular anomalies. *Egypt J Radiol Nucl Med* 48:467–478. <https://doi.org/10.1016/j.ejrmn.2017.02.003>
29. Ishihara A, Funabashi N, Ozawa K et al (2016) The use of whole thoracic ECG-gated MDCT for the de novo diagnosis of isolated patent ductus arteriosus in middle aged or older subjects. *Int J Cardiol* 224:62–64. <https://doi.org/10.1016/j.ijcard.2016.08.335>
30. Leschka S, Oechslin E, Husmann L et al (2007) Pre- and postoperative evaluation of congenital heart disease in children and adults with 64-section CT. *Radiographics* 27:829–846. <https://doi.org/10.1148/rg.273065713>
31. Juneja M, Doshi D, Sahoo S et al (2014) Incidence of aortopulmonary collaterals in patients of Tetralogy of Fallot with pulmonary atresia & correlation with pulmonary artery anatomy. *Indian Heart J* 2:549–50. <https://doi.org/10.1016/j.ihj.2014.10.139>
32. Guruprasadh Ch, Kushaljit SS, Akshay KS et al (2012) Correlation of 64 row MDCT, echocardiography and cardiac catheterization angiography in assessment of pulmonary arterial anatomy in children with cyanotic congenital heart disease. *Eur J Radiol* 81:4211–4217. <https://doi.org/10.1016/j.ejrad.2012.08.010>
33. Sen S, Rao SG, Kulkarni S (2016) Rare associations of tetralogy of Fallot with anomalous left coronary artery from pulmonary artery and totally anomalous pulmonary venous connection. *Cardiol Young* 26:1017–1020. <https://doi.org/10.1017/S1047951116000342>
34. Türkvtan A, Tola HT, Kutlutürk N et al (2017) Low-dose computed tomographic imaging of partial anomalous pulmonary venous connection in children. *World J Pediatr Congenit Heart Surg* 8:590–596. <https://doi.org/10.1177/2150135117723903>
35. Chan SS, Whitehead KK, Kim TS et al (2015) Repaired tetralogy of Fallot with coexisting unrepaired partial anomalous pulmonary venous connection is associated with diminished right ventricular ejection fraction and more severe right ventricular dilation. *Pediatr Radiol* 45:1465–1471. <https://doi.org/10.1007/s00247-015-3358-0>
36. Romeih S, Kaoud A, Hashem M et al (2021) A quantitative assessment of aorta root rotation in patients with tetralogy of Fallot evaluated by MSCT. *Sci Rep* 11:1–7
37. Kemper AR, Mahle WT, Martin GR et al (2011) Strategies for implementing screening for critical congenital heart disease. *Pediatrics* 128:e1259–1267. <https://doi.org/10.1542/peds.2011-1317>
38. Siripornpitak S, Ratanaporn P, Pongsak K et al (2013) Cardiac CT angiography in children with congenital heart disease. *Eur J Radiol* 82:1067–1082. <https://doi.org/10.1016/j.ejrad.2011.11.042>
39. Carine VA, Emmanuel LB, Jean FP et al (2011) Diagnostic accuracy of dual-source multislice computed tomographic analysis for the pre-operative detection of coronary artery anomalies in 100 patients with tetralogy of Fallot. *J Thorac Cardiovasc Surg* 142:120–126. <https://doi.org/10.1016/j.jtcvs.2010.11.016>
40. Dillman JR, Hernandez RJ (2009) Role of CT in the evaluation of congenital cardiovascular disease in children. *Am J Roentgenol* 192:219–231. <https://doi.org/10.2214/AJR.09.2382>
41. Eltatawy DN, Elsharawy FA, Elbarbary AA et al (2021) Multi-detector computed tomography (MDCT) as a diagnostic tool in assessment of thoracic aortic anomalies in pediatric patients. *Egypt J Radiol Nucl Med* 52:1–10

Publisher's Note

Springer Nature remains neutral with regard to jurisdictional claims in published maps and institutional affiliations.

Submit your manuscript to a SpringerOpen® journal and benefit from:

- Convenient online submission
- Rigorous peer review
- Open access: articles freely available online
- High visibility within the field
- Retaining the copyright to your article

Submit your next manuscript at ► [springeropen.com](https://www.springeropen.com)